

Effect of the Carbonization Temperature on the Properties of Biochar Produced from the Pyrolysis of Crop Residues

Zhaoxia Liu,^{1,a,b} Wenjuan Niu,^{1,a,*} Heying Chu,^b Tan Zhou,^a and Zhiyou Niu^{a,*}

Biochar, a carbon-rich product, can be obtained from crop residues via pyrolysis. Its properties may vary widely depending upon the pyrolysis conditions and feedstock type. Physicochemical properties were studied for biochars produced from rice straw, wheat straw, corn stover, rape stalk, and cotton stalk pyrolyzed at 300 °C to 700 °C. At higher pyrolysis temperatures, the carbon content, pH, and electrical conductivity of the biochars slightly increased, while the O/C and H/C ratios decreased. The pH values had a strong negative linear correlation with the H/C ratio. Higher carbonization temperatures resulted in larger pores and increased the aromatic/aliphatic carbon ratio in the biochars. The oxygen functional groups in the biochars, such as -COOH and -OH, decreased with an increasing carbonization temperature. The combustion performance of the biochars varied with the carbonization temperature because of the differences in the physicochemical compositions of the biochars. Additionally, the crop residue types also influenced the physicochemical properties. The cotton stalk biochar had the highest fixed carbon content and lowest H/C ratio, and thus can be used as a solid biofuel. The rice straw biochar, which had the highest N and O contents, may be a potential soil amendment.

Keywords: Biochar; Crop residues; Property; Carbonization temperature

Contact information: a: Key Laboratory of Agricultural Equipment in Mid-lower Yangtze River, Ministry of Agriculture, College of Engineering, Huazhong Agricultural University, 430070 Wuhan, P. R. China; b: College of Mechanical and Electronic Engineering, Tarim University, 843300, Alar, P. R. China; *Corresponding authors: nzhy@mail.hzau.edu.cn; niuwenjuan234@mail.hzau.edu.cn; 1: These authors contributed equally to this work

INTRODUCTION

Pyrolysis technology is an effective way to utilize crop residues and solve environmental pollution problems caused by the burning of crop residues in the field. Additionally, pyrolysis products can be used as alternative renewable energy sources to fossil fuels (Clare *et al.* 2015). In 2010, a total of 842 million metric tons of crop residues were produced in China, which mainly included rice straw, wheat straw, corn stover, rape stalk, and cotton stalk (Peng *et al.* 2014). Crop residues may be burnt in the fields or directly incorporated into soils by farmers to increase the organic carbon content (Villamil *et al.* 2015). The burning of crop residues is a major contributor to carbon dioxide emissions (Murali *et al.* 2010). The most efficient way to solve this problem may be the conversion of crop residues into biochars by pyrolysis and carbonization. The solid pyrolysis products of crop residues are biochars, which contain char, ash, and unchanged biomass materials. Biochar can be used as a fuel, for carbon sequestration, as activated carbon, and soil amendment to reduce greenhouse gas emissions (Lehmann *et al.* 2006;

Wu *et al.* 2013). The pore structure and contents of nitrogen (N), phosphorus (P), and potassium (K) in biochar make it an effective material to improve soil quality (Sohi *et al.* 2009).

The physicochemical properties of biochars vary with the pyrolysis conditions and type of crop residue. Among the pyrolysis parameters, the carbonization temperature is thought to remarkably influence the final properties of the biochar because of the release of volatile compounds and decomposition of organic compounds (Zhang *et al.* 2015b). It has been previously reported that for wheat straw, the biochar yield, surface oxygen (O)-containing groups, and contents of hydrogen (H), N, and O decreased with an increasing carbonization temperature (Zhang *et al.* 2015a). Biochars have been generated from manure, crop straw, nutshell, wood, and grass under various experimental conditions (Cantrell *et al.* 2012; Jeong *et al.* 2016). Biochars obtained from manures have a high content of ash because of their high levels of inorganic compounds, while wood and grass biochars have a low nutrient content, are carbon-rich, and have a higher rate of CO₂ adsorption (Cantrell *et al.* 2012; Ghani *et al.* 2013). Crop residues are composed of multiple components, such as cellulose, lignin, and hemicellulose, and the properties of the resulting biochars can vary remarkably with the type of crop residue. Therefore, it is highly necessary to characterize the physical and chemical properties of biochars made from various crop residues.

The physicochemical characteristics of crop residue biochars have been studied by a few researchers (Fu *et al.* 2012; Wu *et al.* 2013), but only a couple crop residues and their pyrolysis products have been studied under various conditions (Lee *et al.* 2010; Zhang *et al.* 2015b). Therefore, it is important to clarify the properties of biochars produced from multiple crop residues under similar pyrolysis conditions. This study investigated the effects of the carbonization temperature and crop residue type on the physicochemical properties of the final biochars. The results are expected to facilitate the production of biochars from crop residues with higher additional values, and lead to the effective and proper utilization of crop residues for different purposes.

EXPERIMENTAL

Biochar Preparation

Rice straw, wheat straw, corn stover, rape stalk, and cotton stalk were collected from Wuhan, Hubei Province in China. The collected crop residue samples were processed according to ASTM E1757-01 (2015). The samples were dried in a forced-air drying oven at 45 °C for 48 h, and then fed into a ZM100 mill (Retsch GmbH & Company, Haan, Germany) and milled to pass through a 0.425-mm sieve. The samples were stored in bags prior to the pyrolysis analysis. Cellulose, hemicellulose, and lignin were measured according to the National Renewable Energy Laboratory method (Sluiter *et al.* 2010). The basic compositions of the crop residues are shown in Table 1. The contents of cellulose, hemicellulose, and lignin in crop residues are 36.04% to 41.69%, 11.48% to 14.41%, and 18.46% to 27.35%, respectively. The cellulose content is the highest in rice straw and the lowest in corn stover. Cotton stalk contains the highest lignin and the lowest hemicellulose.

Approximately 30.0 g of crop residue were loaded into a square crucible (120 mm × 80 mm × 40 mm) and then placed into a tube furnace. Nitrogen was passed through the furnace for 30 min to remove the air and provide an inert gas atmosphere for pyrolysis.

The crop residues were pyrolyzed at 300 °C, 350 °C, 400 °C, 450 °C, 500 °C, 550 °C, 600 °C, 650 °C, and 700 °C. The heating rate was 10 °C/min and the holding time was 30 min. Then, the crucible with the product was naturally cooled to room temperature inside of the furnace. The biochar was immediately weighed after it was removed from the furnace. Each experiment was performed in duplicate.

Table 1. Chemical Composition of the Five Crop Residues

Crop Residue	rice straw	wheat straw	corn stover	rape stalk	cotton stalk
Cellulose (%)	41.69	38.7	36.04	39.98	39.28
Hemicellulose (%)	14.41	17.63	13.36	13.23	11.48
Lignin (%)	20.53	22.41	22.39	18.46	27.35
Ash (%)	13.77	8.66	5.69	7.17	4.07
VM (%)	67.71	71.02	72.98	71.69	72.23
FC (%)	12.64	14.19	14.3	15.15	16.7
C (%)	38.62	37.83	41	39.7	36.71
H (%)	6.1	10.18	7.17	7.63	7.77
N (%)	1.3	1.31	0.99	1.13	1.19
O (%)	32.88	36.74	33.24	38.8	41.55
H/C	1.9	3.23	2.1	2.31	2.54
O/C	0.64	0.73	0.61	0.73	0.85

VM – volatile matter; FC – fixed carbon; H/C – ratio of H to C; O/C – ratio of O to C

Biochar Characteristics

Biochar yield

A number of physicochemical properties of the obtained biochars were determined. Each resulting biochar was characterized for its basic properties, including the pH, electrical conductivity (EC), proximate composition, and elemental composition. The surface functional groups and porosities were investigated using scanning electron microscopy (SEM), Fourier transform infrared (FTIR) spectroscopy, and X-ray photoelectron spectroscopy (XPS).

The biochar yield (dry basis, %) was calculated using Eq. 1,

$$\text{Biochar yield (\%)} = \frac{m_a \text{ (g)}}{m_b \text{ (g)}} \times 100\% \quad (1)$$

where m_a refers to the weight (g) of the sample after pyrolysis and m_b is the weight (g) of the sample before pyrolysis.

Proximate and ultimate analyses

The proximate analysis was conducted according to ASTM D1762-84 (2001). The ash content in the biochar samples was determined by the combustion of the biochar at 750 °C to a constant weight for 6 h. The volatile matters were analyzed at 900 °C after 6 min of combustion in a muffle furnace. The fixed carbon content in the biochar was calculated with Eq. 2,

$$\text{Fixed Carbon(\%)} = 100\% - \text{Volatile Matter(\%)} - \text{Ash(\%)} \quad (2)$$

The carbon (C), H, N, sulfur (S), and O contents were determined by an element analyzer (EA3000, EuroVector, Milan, Italy) *via* combustion at 980 °C using the CHNS and O methods.

pH, electrical conductivity and metals

The pH and EC of the biochars were measured with a suspension, which contained 0.40 g of dry biochar sample dispersed in 8 mL of deionized water, using a shaking table at a constant temperature of 25 °C for 24 h. Metal analysis was performed for K, Na. The analysis was performed by using wet acid digestion (conc. H₂SO₄ + 30% H₂O₂) and determined by AA-6300C atomic absorption spectrometry (Shimadzu, Kyoto, Japan).

Fourier transform infrared spectra

The FTIR spectra of the biochars were obtained by a Vertex 70 FTIR spectrometer (Bruker, Ettlingen, Germany). All of the samples were dried at 105 °C for 24 h before being homogenized into a fine powder using a ball mill. Then, the biochars were mixed with KBr at a fixed ratio to fabricate translucent discs.

Scanning electron micrographs and X-ray photoelectron spectra

The surface morphologies of the biochars were investigated using field-emission SEM (Nova NanoSEM 450, Eindhoven, Netherlands). The XPS spectra were obtained with an AXIS-Ultra DLD-600W spectrometer (Kratos Analytical Ltd, Shimadzu, Kyoto, Japan) using 1000 eV to 1500 eV of X-ray radiation as the XPS excitation source. The binding energy for C1s was assigned to 284.9 eV. The relative contents of C, O, and N on the surface of biochars were calculated from XPS data.

Thermogravimetric analysis

A thermogravimetric analyzer (SDT Q600 thermal analyzer, TA Instruments, New Castle, USA) was used to analyze the combustion characteristics. A 10-mg sample was accurately weighed in an alumina crucible and placed into the SDT Q600 analyzer with dry air as the carrier gas at a flow rate of 100 mL/min. The temperature was increased from room temperature to 900 °C at a rate of 20 °C/min. All of the analyses were conducted in triplicate. Meanwhile, the pyrolysis process of cellulose, hemicellulose and lignin in nitrogen atmosphere was analyzed. The carrier gas was high purity nitrogen (99.999 %), and the flow rate was 100 mL/min. The pyrolysis temperatures were from room temperature to 900 °C.

RESULTS AND DISCUSSION

Biochar Yields

The biochar yields of the five crop residues ranged from 30.51% to 75.66% (Fig. 1). For all of the crop residues, the biochar yield decreased sharply when the temperature was increased from 300 °C to 400 °C, and it decreased more slowly at temperatures of 450 °C and above. From the TG-DTG curves of cellulose, hemicellulose, and lignin, the hemicellulose was decomposed from 200 °C to 300 °C. Cellulose was decomposed from 300 °C to 380 °C. The decomposition of lignin occurred from 200 °C to 500 °C (Fig. 1

c). The crop residues were decomposed, and some vapors, including CO₂, CO, H₂, CH₄, and C_nH_m, were released with an increase in the temperature, and also the yields of these gases increased with the increase of carbonization temperature (Antal 2003; He *et al.* 2017). The biochar yields at 400 °C were approximately half of those obtained at 300 °C.

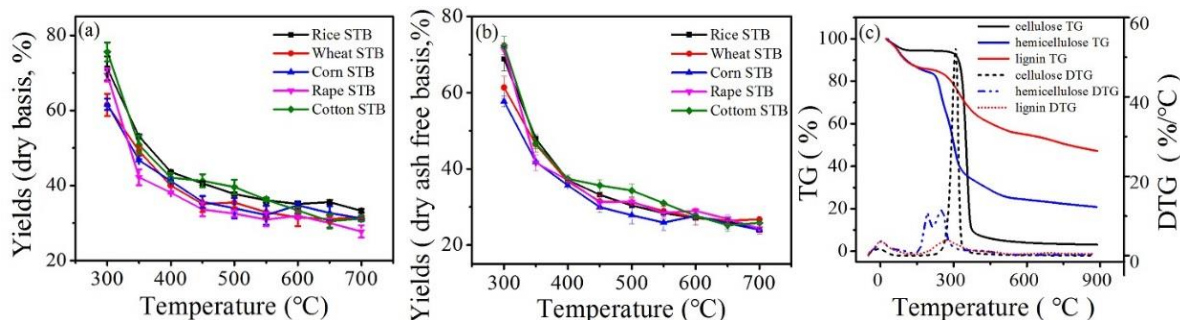


Fig. 1. Biochar yields of dry basis (a) and dry ash free basis (b) at different carbonization temperatures, and TG-DTG curves (c) of cellulose, hemicellulose, and lignin

Some variations were observed in the biochar yields (dry basis) among different crop residues. The biochar yields may have varied depending on the different contents of cellulose, hemicellulose, lignin, and inorganic mineral components in the different crop residues (Niu *et al.* 2016). The biochar yield of the cotton stalk was highest at 300 °C, which may have been because of the relatively higher lignification degree of the cotton stalk (Table. 1). The pyrolysis products of the lignin contained more residual solid char because of the large number of benzene rings in the lignin structure and a great number of benzene-containing radicals that were generated from pyrolysis further developed into polycyclic aromatic compounds and formed the char (Chen and Cai 2009). From 400 °C to 550 °C, the cotton stalk and rice straw had slightly higher biochar yields, while the rape stalk had the lowest biochar yield. However, the biochar yields (dry ash free basis) of the cotton stalk were the highest, while the corn stover biochar yields were the lowest. Interestingly, at 600 °C to 700 °C, the rice straw had the highest biochar yield (dry basis), but the differences in the biochar yields (dry ash free basis) at 600 °C to 700 °C were small. The highest yields (dry basis) of the rice straw biochars at the temperatures over 600 °C were mainly because of the accumulation of inorganic mineral components.

Biochar Characterization

Proximate analysis

With an increasing carbonization temperature, the volatile matter contents of the biochars gradually decreased, while the ash content of the biochars increased (Table 2). Consistent with the volatile matter in the raw crop residues, the volatile matters in the corn stover and cotton stalk biochars were higher than those in the wheat straw and rice straw biochars. The rape stalk biochar had the highest volatile matter content (Tables 1 and 2). The highest ash content was observed in the rice straw biochar, which ranged from 13.77% at 300 °C to 37.91% at 700 °C. This may have been caused by the compositional changes that resulted from the interaction between the organic and inorganic components during rice straw pyrolysis (Tables 1 and 2) (Jindo *et al.* 2014). The lowest ash content was observed in the rape stalk biochar. The fixed carbon contents

in this study ranged from 47.51% to 71.69% (Table 2). Generally, the fixed carbon contents of the biochars increased when the temperature was increased from 300 °C to 600 °C, and the biochars with a lower ash content had a higher fixed carbon content. The contents of fixed carbon between 600 °C and 700 °C were slightly decreased, and this may be caused by the increase of crystallinity and content of calcite in the biochars produced at 700 °C (Yuan *et al.* 2011). The fixed carbon content in the rice stalk biochar was remarkably lower than that in the other biochars, which may have been because of its higher ash content (Table 2).

Table 2. Proximate and Ultimate Analyses of the Biochars

Biochar	Ash (%)	VM (%)	FC (%)	C (%)	H (%)	N (%)	O (%)	S (%)	H/C	O/C
Rice STB-300	16.57	62.35	21.08	48.33	5.34	2.58	24.91	0.52	1.33	0.39
Rice STB-400	26.71	32.21	41.09	54.28	3.65	2.15	15.64	0.47	0.81	0.22
Rice STB-500	30.49	23.60	45.92	54.31	3.45	1.68	11.87	0.47	0.76	0.16
Rice STB-600	33.36	16.34	50.30	56.85	2.27	0.87	7.89	0.45	0.48	0.10
Rice STB-700	37.91	14.01	48.08	55.28	1.88	1.08	6.84	0.44	0.41	0.09
Wheat STB-300	12.64	59.89	27.47	47.51	6.4	0.80	29.65	0.75	1.62	0.47
Wheat STB-400	16.26	33.79	49.95	58.74	5.30	0.95	15.32	0.77	1.08	0.20
Wheat STB-500	19.54	20.75	59.71	61.47	3.84	0.73	8.17	0.83	0.75	0.10
Wheat STB-600	20.99	13.88	65.14	65.18	2.84	0.49	5.73	0.89	0.52	0.07
Wheat STB-700	22.65	14.38	62.97	65.39	2.91	0.50	7.17	0.89	0.53	0.08
Corn STB-300	11.69	61.16	27.15	53.22	5.01	2.61	23.97	0.58	1.13	0.34
Corn STB-400	18.45	39.33	42.22	58.09	3.84	2.69	15.15	0.58	0.79	0.20
Corn STB-500	22.68	24.25	53.07	59.72	2.49	2.43	10.01	0.53	0.50	0.13
Corn STB-600	25.05	19.89	55.05	61.76	2.16	1.73	7.52	0.54	0.42	0.09
Corn STB-700	27.58	21.28	51.13	60.00	1.83	0.93	9.64	0.53	0.37	0.12
Rape STB-300	8.18	69.73	22.09	52.64	6.75	0.88	27.4	0.88	1.54	0.39
Rape STB-400	14.04	35.45	50.51	65.89	5.35	0.86	17.34	1.13	0.97	0.20
Rape STB-500	16.32	25.78	57.90	71.69	3.39	1.08	10.76	1.27	0.57	0.11
Rape STB-600	17.29	25.12	57.59	70.92	2.36	0.665	8.57	1.28	0.40	0.09
Rape STB-700	18.74	24.54	56.72	70.80	2.04	0.61	10.72	1.29	0.35	0.11
Cotton STB-300	8.32	57.02	34.66	51.56	4.70	1.40	35.36	0.59	1.09	0.51
Cotton STB-400	14.82	40.75	44.43	63.69	3.59	1.34	17.86	0.65	0.68	0.21
Cotton STB-500	16.94	27.76	55.30	69.1	2.57	1.01	13.71	0.68	0.45	0.15
Cotton STB-600	20.53	15.72	63.74	70.79	1.70	0.72	8.12	0.70	0.29	0.09
Cotton STB-700	20.59	17.76	61.65	65.66	1.94	0.28	9.32	0.72	0.35	0.11

Rice STB, rice straw biochar; Wheat STB, wheat straw biochar; Corn STB, corn stover biochar; Rape STB, rape stalk biochar; Cotton STB, cotton stalk biochar. The values following the biochar labels denote the temperature at which the material was pyrolyzed

Ultimate analysis

An ultimate analysis of the biochars was performed, and the results are shown in Table 2. The pyrolysis resulted in an increase in the C and N contents compared with the corresponding crop residues (Tables 1 and 2). The C content in the biochars increased with an increasing carbonization temperature, while the N content decreased and the C/N

ratios ranged from 20 to 200. The H and O contents decreased with an increasing carbonization temperature. The loss of H and O in the biochars was mainly attributed to the cleavage of oxygenated bonds during the heating process (Fu *et al.* 2012). The S contents in the wheat straw, rape stalk, and cotton stalk biochars increased noticeably with an increasing carbonization temperature, but those in the rice straw and corn stover biochars decreased. The decrease of S content in the biochars at 700 °C was thought to be due to the decomposition or evaporation of alkali metal sulfates (Lith *et al.* 2006, 2008).

The H/C of the biomass without burning such as cellulose and lignin was about 1.5, while the H/C of black carbon was lower than 0.2. The H/C of the biochar prepared at the temperature above 400 °C was ≤ 0.5 (Skjemstad and Graetz 2003). The decrease in H/C and O/C ratio was indicative of the formation of structures containing condensed carbons such as the aromatic rings. So the H/C and O/C was usually used to determine the degree of aromatics of biochars (Wu *et al.* 2012). The H/C and O/C molar ratios of different biochars are shown in Table 2. Regardless of the type of biochar, the H/C and O/C molar ratios had similar values. Both the H/C and O/C values for all of the biochar types were slightly lower than those of the crop residues. The H/C and O/C ratios decreased with an increasing carbonization temperature. The decrease in the ratios was possibly caused by the loss of volatile organic compounds and an increase in dehydrogenation and deoxygenation reactions over the course of heating (Xiao *et al.* 2016). The molar O/C ratio of biochar could partially indicate its surface hydrophilicity (Chun *et al.* 2004). The lower O/C ratios of the biochars at higher carbonization temperatures implied higher hydrophobicity of the biochars.

By comparing the biochars from different crop residues, it was found that the rape stalk biochar had the highest C, H, and S contents, and the rice straw biochar had the highest N and O contents. The H/C ratio was the lowest in the cotton stalk biochar and the highest ratio was in the wheat straw biochar for the carbonization temperature of 300 °C to 600 °C. The H/C atomic ratios seemed to be stable at 600 °C and 700 °C in the rice straw, corn stover, and rape stalk biochars, whereas slight increases were observed in the wheat straw and cotton stalk biochars for the same conditions.

pH and electrical conductivity analysis

Figure 2 shows the pH and EC of the biochars. The pH values of the biochars in water ranged from slightly acidic (6.3) to alkaline (10.6). The pH increased considerably with the carbonization temperature from 300 °C to 550 °C, and then it slowly increased when the carbonization temperature was over 550 °C.

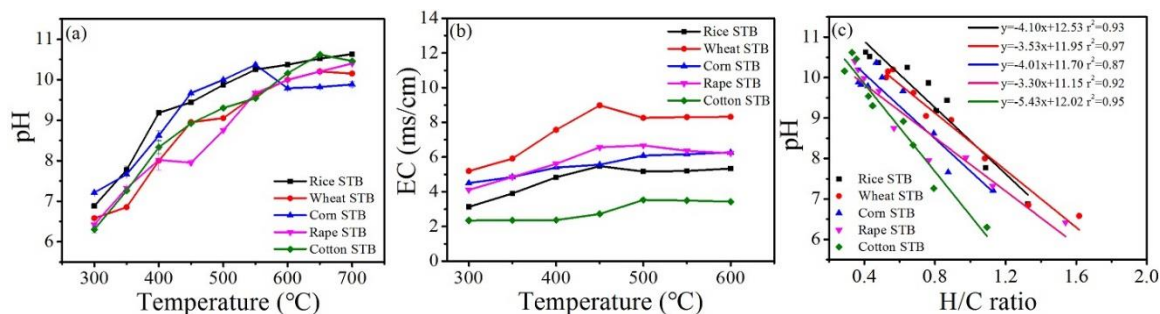


Fig. 2. Impact of the pyrolysis temperature on the pH (a) and EC (b) of the biochars; and relationship between the H/C ratio and pH (c)

These changes might be associated with the dehydration of the crop residues and a progressive loss of acidic surface groups during thermal treatment.

The biochars produced at higher carbonization temperatures with a lower H/C ratio had a relatively higher pH value, which indicated that the pH of the biochar was related to the carbonization degree. The lower H/C ratio of 0.1 for lignite coke was in accordance with the dominance of graphite-like domains, and the lower H/C ratio at higher temperatures indicated the biochar had a higher carbonization degree (Knicker *et al.* 2005). The development of alkaline pH values was determined by the extent of the biochar carbonization that resulted from the concentration of basic inorganic components, such as inorganic carbonates, in the biochar at high temperatures and formation of insoluble salts during pyrolysis (Yuan *et al.* 2011). The carbonates in the biochar and organic anions on the biochar surface were the main alkaline components in the biochars. With an increasing pyrolysis temperature, the content of carbonates in the biochars increased, while the content of organic anions on the biochar surface decreased. The contribution of carbonates to the alkalinity of the biochars increased with the pyrolysis temperature (Yuan *et al.* 2011). The alkaline biochar produced under higher temperatures may be used to improve acidic soils (Venegas *et al.* 2015).

The pH values had a strong negative linear correlation with the H/C ratio of the same species of biochars, which has also been observed for other biochars (Yargicoglu *et al.* 2015). The correlation coefficient (r^2) values of the curves were all above 0.90, except for the corn stover biochar curve (0.87). The maximum and minimum slopes of the fitting curve were assigned to the cotton stalk and rape stalk biochars, respectively.

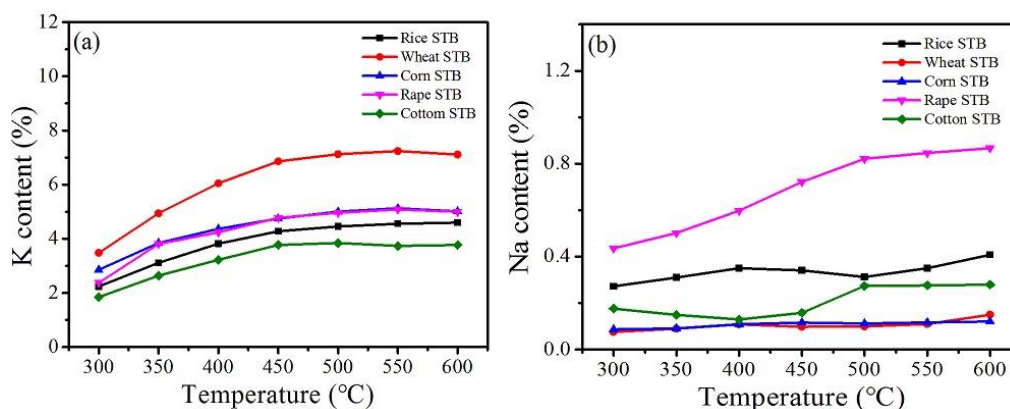


Fig. 3. Contents of K (a) and Na (b) in the biochars prepared at different temperatures

The EC is an electrochemical property that can reflect the degree of salinity in the biochar. The biochars were characterized with a wide EC range from 2.34 mS/cm for the cotton biochar to 9.12 mS/cm for the wheat straw biochar (Fig. 2b). The EC of the biochars increased with the carbonization temperature first, and then tended to be steady when the carbonization temperature was over 500 °C (Fig. 2b). The increase of EC was due to the loss of volatile compounds, which resulted in an increased mineral element concentration (Cantrell *et al.* 2012). These results were not consistent with those described by Pituello *et al.* (2015), who found that the biochars derived from sewage sludge, municipal organic waste, cattle manure, and silage digestates had higher EC values at low and high temperatures. The highest EC of wheat straw biochar was related to its highest K content (Fig. 3a), while the cotton biochars with the lowest K contents

showed the lowest EC. The rape stalk biochars with higher K and Na contents showed a higher EC value than those of rice straw, wheat straw and cotton stalk biochars (Figs. 2b and 3b.). The results were consistent with that from Cantrell's studies (Cantrell *et al.* 2012). The low EC values indicated that the biochars had a low salinity, and thus would not have negative effects on plants and soil organisms and can be safely used to improve the quality of soils (Buss *et al.* 2016).

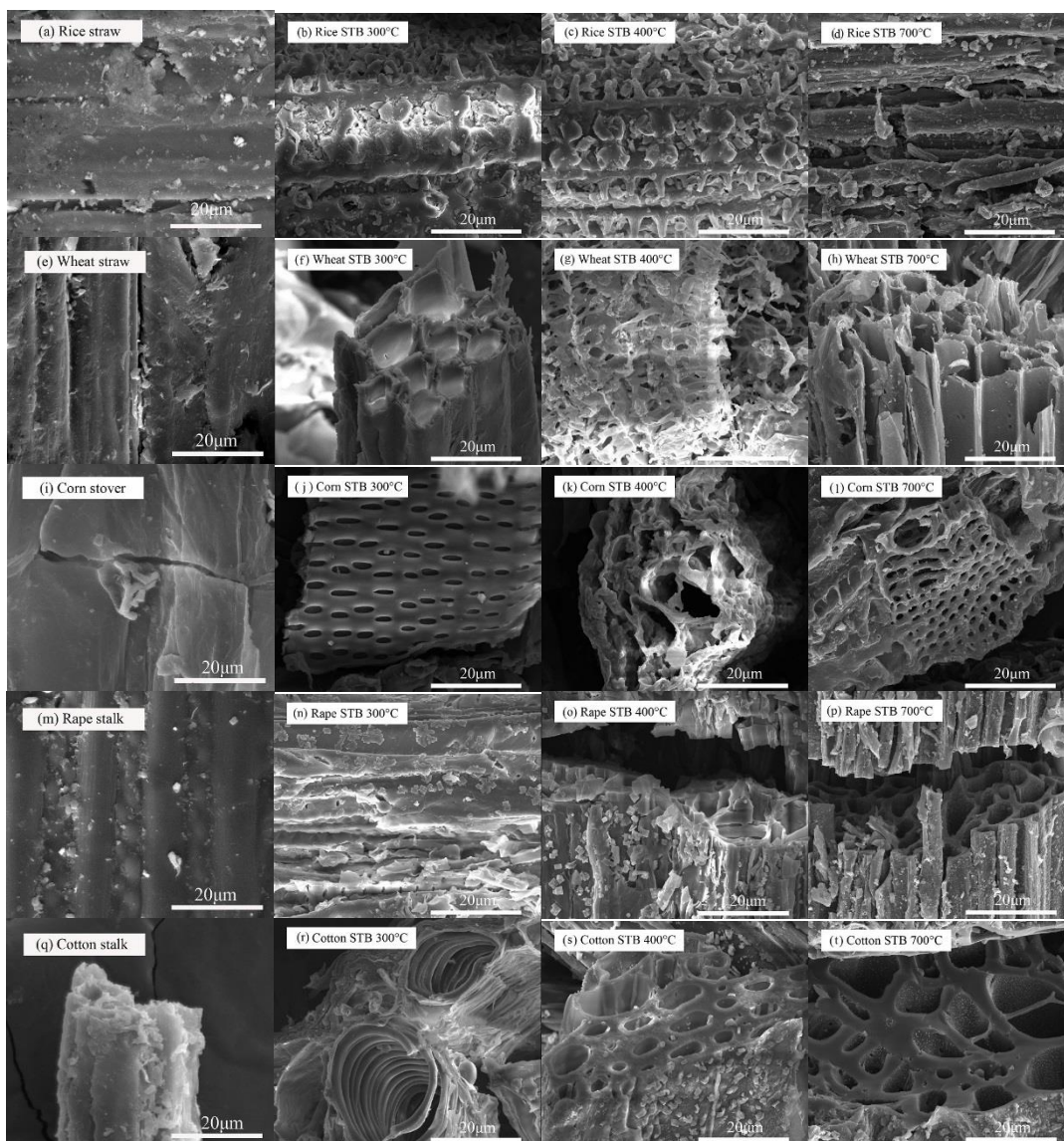


Fig. 4. SEM micrographs of the samples: (a) rice straw, (b) rice STB-300 °C, (c) rice STB-400 °C, (d) rice STB-700 °C, (e) wheat straw, (f) wheat STB-300 °C, (g) wheat STB-400 °C, (h) wheat STB-700 °C, (i) corn stover, (j) corn STB-300 °C, (k) corn STB-400 °C, (l) corn STB-700 °C, (m) rape stalk, (n) rape STB-300 °C, (o) rape STB-400 °C, (p) rape STB-700 °C, (q) cotton stalk, (r) cotton STB-300 °C, (s) cotton STB-400 °C, (t) cotton STB-700 °C with a holding time of 30 min and heating rate of 10 °C /min

Scanning electron microscopy analysis

The surface morphologies of the crop residues and biochars were analyzed using SEM (Fig. 4). The SEM images clearly showed the development of the pores in the biochars from the original fiber structures in the crop residues. Figures 4a, 4e, 4i, 4m, and 4n showed that the surfaces of raw materials were smooth and close texture. The crop residue feedstocks were incompletely decomposed at 300 °C, and the images showed that the samples retained their physical form with particles on the surfaces and no visible porosity (Figs. 4a, 4b, 4e, 4f, 4i, 4j, 4m, 4n, 4q, and 4r). With an increasing temperature, the original structure was damaged and some minipores were observed in the pore walls of the biochars. The pore diameters were slightly larger and there were more particles on the surfaces of the biochars produced at higher temperatures (Figs. 4c, 4g, 4k, 4o, and 4s). Distinct honeycomb-like macropores were observed in the rape stalk and cotton stalk biochars (Figs. 4o, 4p, 4s, and 4t), and straight pipe-like pores were found in the corn stover biochars (Fig. 4l). The existence of pores on the biochar is important for microbial activity and the reservation of soil nutrients. Also, the presence of macropores on the biochar provides a suitable space for clusters of microorganisms to inhabit (Quilliam *et al.* 2013).

Fourier transform infrared spectroscopy analysis

The FTIR spectra of the biochars with the carbonization temperature and crop residue type as the variables are presented in Figs. 5a and 5b, respectively. The FTIR spectra of the biochars showed the changes to the functional groups on the surfaces of the biochars. The assignments of the peaks and adsorption bands of the spectra in the biochars are shown in Table 3.

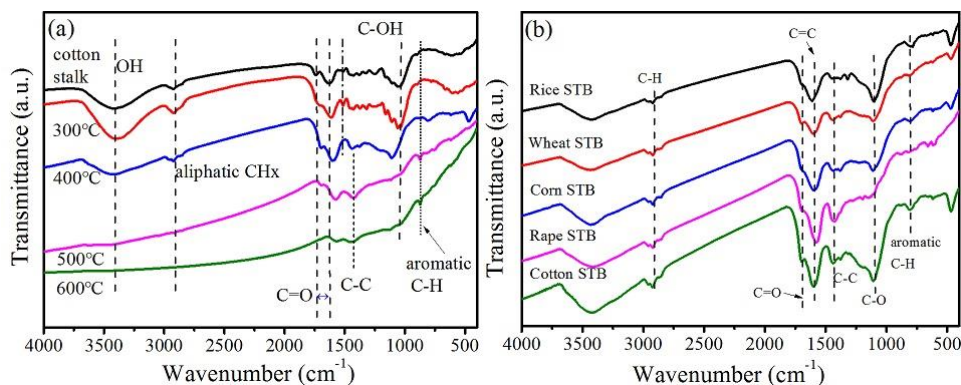


Fig. 5. FTIR analysis of the cotton stalk biochars produced at different temperatures (a) and biochars obtained from the five crop residues at 400 °C (b)

After heating to 300 °C, the increase in the peak intensity of the C=O stretching vibrations between 1609 cm^{-1} and 1738 cm^{-1} , represented the formation of ketones, quinones, carboxyls, and aromatic components (Chun *et al.* 2004). Meanwhile, the absorbance peak of the C-O stretching at 1030 cm^{-1} associated with cellulose, hemicellulose, and lignin (Pastorova *et al.* 1994) decreased. Heating to 400 °C resulted in more substantial chemical transformations. The absorbance peak of the aliphatic C-H stretching (mostly at 2908 cm^{-1}) (Yuan *et al.* 2011) decreased slightly, but it did not disappear, which indicated that the aliphatic structures were heat resistant. The intensity of the wide adsorption band detected at 3500 cm^{-1} to 3200 cm^{-1} , which was assigned to the O-H stretching vibration of acid or alcohol structures (Wu *et al.* 2012), decreased at

400 °C. When the carbonization temperature increased up to 500 °C, the characteristic peaks related to oxygenated substituents, aliphatic C stretching progressively decreased. The peaks near 885 cm⁻¹ for aromatic C-H in the spectra (Yao *et al.* 2011) of the biochars obtained above 500 °C indicated the formation of aromatic compounds. The shapes of the spectra curve became much simpler at 700 °C compared with those obtained at lower temperatures.

Differences were observed in the FTIR spectra of the different biochars obtained at 400 °C (Fig. 5b). Bands reflecting undecomposed cellulosic and ligneous C (mostly at 1030 cm⁻¹ to 1100 cm⁻¹) were observed in all of the biochar spectra, and the intensity of the peak in the cotton stalk biochar spectra was higher than that of the other four biochars. The peak at 1440 cm⁻¹ is caused by C-C skeleton vibration of the aromatic ring, and the intensities of the peaks in the rape and cotton stalk biochar spectra were higher than those in the spectra of the other biochars (Hamzah *et al.* 2013). The peak at 1030 cm⁻¹, which corresponded to C-O stretching vibrations in cellulose and hemicellulose, also showed component differences in the biochars, and the intensity of the peak in the cotton stalk biochar spectra was higher than in the spectra of the other biochars. The O-containing functional groups may have increased the hydrophilicity of the biochar surfaces and reduced the sorption of hydrophobic organic compounds (Jin *et al.* 2017). The increased cation exchange capacity in biochar-rich soils is closely related to the formation of O- and H-containing functional groups, such as carboxylic and phenolic groups, and the relative decrease in the C content on the biochar surface (Wiedner *et al.* 2015).

Table 3. Assignment of the Characteristic Vibrations to the Peaks in the Biochar FTIR Spectra

Wavenumber (cm ⁻¹)	Functional Group Vibration
3600 to 3100	O-H stretching of hydroxyl groups (Wu <i>et al.</i> 2012)
2950 to 2850	C-H stretching of aliphatic CH _x (Taherymoosavi <i>et al.</i> 2016, Yuan <i>et al.</i> 2011)
1740 to 1700	C=O stretching of carboxyls (Chun <i>et al.</i> 2004)
1630 to 1600	C=O stretching in quinones and ketonic acids (Chun <i>et al.</i> 2004)
1440	C-C skeleton vibration of the aromatic ring (Hamzah <i>et al.</i> 2013)
1375	aliphatic deformation of CH ₂ or CH ₃ groups or O-H bending of phenolic-OH (Aslan-Sungur <i>et al.</i> 2013)
1110 to 1030	C-O-C stretching vibrations in cellulose and hemicellulose (Pastorova <i>et al.</i> 1994)
900 to 750	C-H bending aromatic CH out-of-plane deformation (Yao <i>et al.</i> 2011)

X-ray photoelectron spectroscopy analysis

X-ray photoelectron spectroscopy measurements were performed on the biochars, which is a powerful technique for obtaining accurate information on the chemical states of the surface elements. The C1s and O1s spectra with peak fitting of their envelopes are shown in Fig. 6. The C1s spectra were fitted to several peaks, including the most intense peak at the binding energy of 285.0 eV, two peaks at approximately 286.5 eV and 287.5 eV, and a relatively weak peak around 289.0 eV, which were assigned to C-C, -C-OR, COOH and COO-, and O=C-O bonds, respectively (Fuertes *et al.* 2013). Similarly, the curve fitting of the O1s peak in the XPS spectra of the biochars showed the existence of three O groups on the biochar surface, including -C=O at 531.5 eV, C-O in carboxylic groups at 533 eV, and -OH functional groups at 535 eV (Srinivasan and Sarmah 2015).

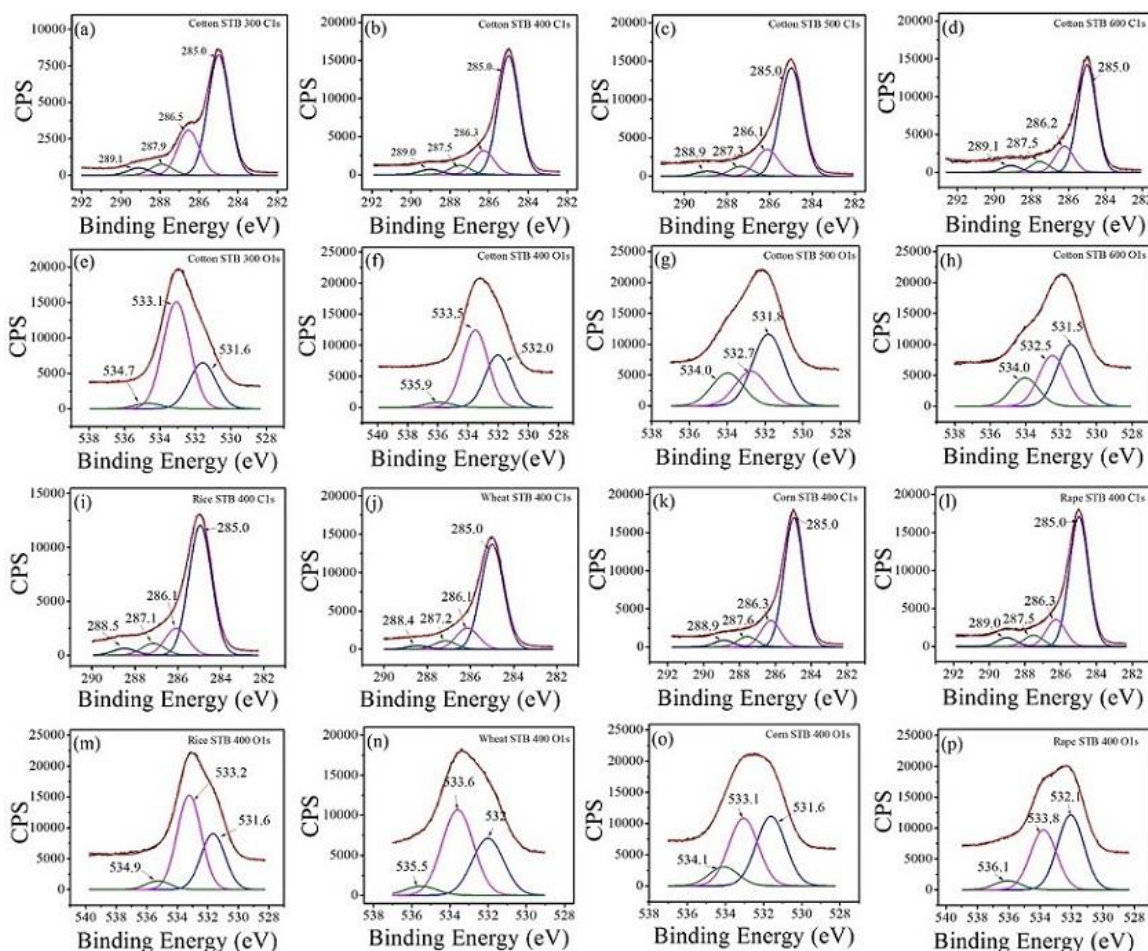


Fig. 6. Curve fitting of the peaks in the XPS spectra of the biochars: C1s peaks of (a) cotton STB-300 °C, (b) cotton STB-400 °C, (c) cotton STB-500 °C, (d) cotton STB-600 °C, (i) rice STB-400 °C, (j) wheat STB-400 °C, (k) corn STB-400 °C, and (l) rape STB-400 °C; O1s peaks of (e) cotton STB-300 °C, (f) cotton STB-400 °C, (g) cotton STB-500 °C, (h) cotton STB-600 °C, (m) rice STB-400 °C, (n) wheat STB-400 °C, (o) corn STB-400 °C, and (p) rape STB-400 °C

As can be seen from the XPS spectra of the cotton stalk biochars (Figs. 6a, 6b, 6c, and 6d), the intensity of the peaks increased with the temperature, except for the peak corresponding to C-O-C bonds at 286.5 eV. The intensity of the peak at 533.1 eV for the O1s spectra was reduced with an increase in the carbonization temperature, which indicated that the amounts of surface C-O-C bonds decreased during pyrolysis (Figs. 6e, 6f, 6g, and 6h). The peak intensity at 531.5 eV for the O1s spectra decreased with an increasing carbonization temperature, which implied that the surface -C=O groups decreased because of the dehydrogenation reactions that occurred during the heating process (Figs. 6e, 6f, 6g, and 6h). This was consistent with the results obtained from the FTIR spectra. In the fitting curves of the biochars obtained at 400 °C from different crop residues (Figs. 6b, 6f, 6i, 6j, 6k, 6l, 6m, 6n, 6o, and 6p), the intensities of the peaks in the C1s and O1s spectra of the rice straw and wheat straw biochars were lower than those of the other biochars, and a displacement of the peaks was also observed. This indicated that the crop residue type also affected the surface groups. The O1s curve of the corn stover biochar showed a higher symmetry than the other biochars (Fig. 6o), which indicated that

the amount of carbonyl (C=O) and carboxylic (C-O) groups on the surfaces of the biochars was similar (Zhang *et al.* 2012), while the weak peak at 534.1 eV indicated the existence of less –OH groups.

The surface element contents and surface polarity of the biochars are shown in Table 4. The surface C content was much higher than the bulk C content for all of the biochars (Tables 2 and 4). The surface C contents of the biochars decreased with an increasing carbonization temperature, except for the rice straw and corn stover biochars, and the bulk C contents of the corresponding biochars increased. The surface O/C ratios of the rice straw and corn stover biochars at 400 °C and 500 °C were higher than those of the other biochars. This indicated the rice straw and corn stover biochars had higher surface polarities, which was possibly because of their higher ash contents. Abundant minerals in biochars result in the exposure of polar groups on the surface, and the higher ash content is probably more favorable for the surface polarity of biochars (Sun *et al.* 2013). The surface O/C ratios of the biochars indicated that the surface was hydrophilic because of the polar groups on the surface, which act as water adsorption centers and facilitate the formation of water clusters on the carbon surfaces (Chun *et al.* 2004). The O-containing functional groups on the biochar surfaces could potentially react with soil minerals, such as Al³⁺, Fe³⁺/Fe²⁺, and Ca²⁺ (Yang *et al.* 2016).

Table 4. Surface Chemical Composition and Surface Polarity of the Biochars

Biochar	Pyrolysis Temperature (°C)	C (%)	N (%)	O (%)	O/C
Rice STB	300	80.61	1.57	17.77	0.23
	400	77.98	1.84	20.01	0.27
	500	75.53	0.99	23.13	0.32
	600	89.29	0.00	10.71	0.13
Wheat STB	300	83.42	0.77	15.75	0.20
	400	84.20	0.77	14.88	0.19
	500	86.15	0.45	13.26	0.16
	600	85.47	0.22	14.24	0.18
Corn STB	300	83.68	2.24	14.02	0.18
	400	81.54	2.71	15.56	0.20
	500	79.58	1.98	18.22	0.24
	600	80.47	1.15	18.15	0.24
Rape STB	300	80.25	0.71	18.97	0.25
	400	83.84	0.73	15.25	0.19
	500	86.21	0.46	13.14	0.16
	600	82.43	0.15	17.31	0.22
Cotton STB	300	79.80	1.67	18.46	0.24
	400	83.87	0.72	15.25	0.19
	500	83.74	0.97	15.06	0.19
	600	84.02	0.45	15.16	0.19

Thermogravimetric analysis

A thermogravimetric (TG) analysis was performed to demonstrate the combustion characteristics of the biochars. Figure 7 shows the TG-differential thermogravimetric (DTG) curves of the biochars in an air atmosphere. Similarities and differences among all of the biochars were observed. The combustion of the biochars in an air atmosphere was divided into three stages (Figs. 7a, 7c, 7e, 7g, and 7i). In the first stage, the biochar had a lower weight loss below 200 °C; in the second stage, the reactions were attributed to thermal decomposition of the volatile matter in the biochars from 240 °C to 360 °C; and

in the third stage, more and larger pore structures were generated with the release of volatile compounds from the biochars when the temperature reached approximately 400 °C. The reactions in the third stage included the emission and combustion of residual volatile compounds and the combustion of fixed carbon. The ignition temperature of the biochars increased with an increase in the carbonization temperature, while the burnout temperature of the biochars first increased and then decreased. Above 500 °C, the burning process was almost completed, and the residue contents increased with an increase in the carbonization temperature. Additionally, the order of the biochars that produced the highest residue contents was as follows: rice straw biochar > corn stover biochar > wheat straw biochar > cotton stalk biochar > rape stalk biochar (Fig. 7k).

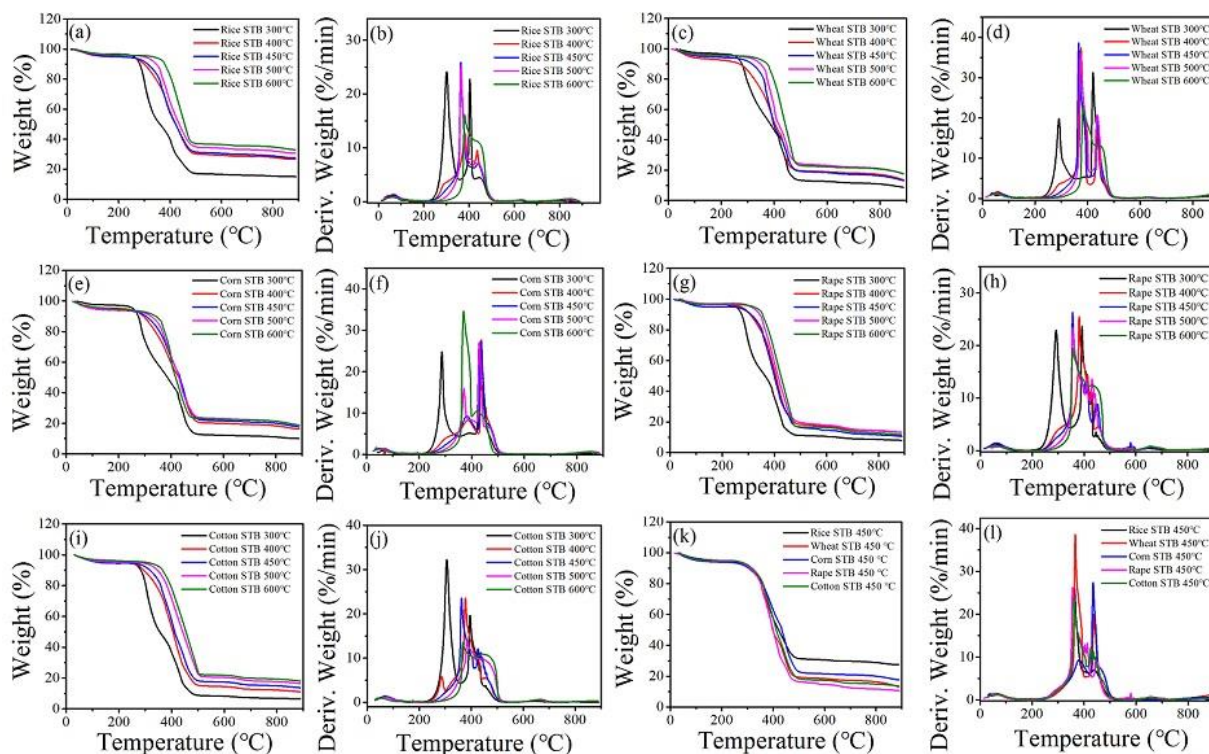


Fig. 7. TG analysis of the biochars: TG curves for (a) rice STB, (c) wheat STB, (e) corn STB, (g) rape STB, (i) cotton STB obtained at different carbonization temperatures (300 °C, 400 °C, 450 °C, 500 °C, 600 °C), and (k) different biochars obtained at 450 °C; DTG curves for (b) rice STB, (d) wheat STB, (f) corn STB, (h) rape STB, (j) cotton STB obtained at different carbonization temperatures (300 °C, 400 °C, 450 °C, 500 °C, 600 °C), and (l) different biochars obtained at 450 °C

The DTG curves widely fluctuated for the different biochars. There were two main peaks in the DTG curves, which corresponded to the maximum weight loss rate from devolatilization and the combustion of fixed carbon (Figs. 7b, 7d, 7f, 7h, and 7j). The temperature corresponding to the maximum weight loss rate of the biochars increased before decreasing with an increase in the carbonization temperature. The maximum weight loss rates for the cotton stalk biochar decreased with an increasing carbonization temperature, while that of the corn stover biochar increased. The maximum weight loss rates for the biochars from the rice straw, wheat straw, and rape stalk first increased, and then decreased at higher carbonization temperatures. Among these five biochars, the wheat straw biochar obtained at 450 °C had the highest maximum weight

loss rate compared with the others. The above results showed that the properties of the biochars obtained above 450 °C in this study were similar to those of coal, which suggested that biochar can potentially be used as a solid fuel (Magdziarz and Werle 2014).

CONCLUSIONS

1. The basic components and physicochemical properties of the biochars generated from five crop residues were characterized. The results showed that the composition of and chemical components in the biochars were remarkably affected by the carbonization temperature during pyrolysis.
2. The increase in the carbonization temperature enhanced the biochar porosity, decreased the biochar yield and H/C and O/C ratios, and increased the pH and EC of the biochars. The carbonization degree and polarity of the biochars increased with an increasing temperature, which implied they have potential applications as long-term C sequestration and a soil amendment. At 400 °C to 500 °C, the biochar yield was a medium amount, and the obtained biochars had a larger amount of the functional O groups and were slightly alkaline. These results indicated that 400 °C to 500 °C may be the optimum temperature range to produce biochars for the amendment of acidic soils.
3. The physicochemical properties of the biochars varied noticeably with the crop residue type. Various components of the biochars from the different initial sources contributed differently to the elemental and structural properties.

ACKNOWLEDGEMENTS

This work was supported by the Natural Science Foundation of China (No. 31701310) and the Agro-Scientific Research Project in the Public Interest (No. 201503135). The authors would also like to acknowledge the Project 2662015QD009 supported by the Fundamental Research Funds for the Central Universities.

REFERENCES CITED

- Antal, M. J. (2003). "The art, science, and technology of charcoal production," *Ind. Eng. Chem. Res.* 42(8), 1619-1640. DOI: 10.1021/ie0207919
- Aslan-Sungur, G., Evrendilek, F., Karakaya, N., Gungor, K., and Kilic, S. (2013). "Integrating ATR-FTIR and data-driven models to predict total soil carbon and nitrogen towards sustainable watershed management," *Research Journal of Chemistry & Environment* 17(6), 5-11.
- ASTM D1762-84 (2001). "Standard test method for chemical analysis of wood charcoal," ASTM International, West Conshohocken, PA.
- ASTM E1757-01 (2015). "Standard practice for preparation of biomass for compositional analysis," ASTM International, West Conshohocken, PA.
- Buss, W., Graham, M. C., Shepherd, J. G., and Mašek, O. (2016). "Suitability of marginal

- biomass-derived biochars for soil amendment,” *Sci. Total Environ.* 547, 314-322. DOI: 10.1016/j.scitotenv.2015.11.148
- Cantrell, K. B., Hunt, P. G., Uchimiya, M., Novak, J. M., and Ro, K. S. (2012). “Impact of pyrolysis temperature and manure source on physicochemical characteristics of biochar,” *Bioresource Technol.* 107, 419-428. DOI: 10.1016/j.biortech.2011.11.084
- Chen, Y., and Cai, H. (2009). “Influence of cellulose and lignin contents on the pyrolysis and combustion feature of sawdust and straw,” *Energ. Eng.* (1), 38-42.
- Chun, Y., Sheng, G., Chiou, C. T., and Xing, B. (2004). “Compositions and sorptive properties of crop residue-derived chars,” *Environ. Sci. Technol.* 38(17), 4649-4655. DOI: 10.1021/es035034w
- Clare, A., Shackley, S., Joseph, S., Hammond, J., Pan, G., and Bloom, A. (2015). “Competing uses for China's straw: The economic and carbon abatement potential of biochar,” *GCB Bioenergy* 7(6), 1272-1282. DOI: 10.1111/gcbb.12220
- Fu, P., Hu, S., Xiang, J., Sun, L., Su, S., and Wang, J. (2012). “Evaluation of the porous structure development of chars from pyrolysis of rice straw: Effects of pyrolysis temperature and heating rate,” *J. Anal. Appl. Pyrol.* 98, 177-183. DOI: 10.1016/j.jaap.2012.08.005
- Fuertes, A. B., Arbestain, M. C., Sevilla, M., Maciá-Agulló, J. A., Fiol, S., López, R., Smernik, R. J., Aitkenhead, W. P., Arce, F., and Macias, F. (2013). “Chemical and structural properties of carbonaceous products obtained by pyrolysis and hydrothermal carbonisation of corn stover,” *Aust. J. Soil Res.* 48(7), 618-626. DOI: 10.1071/SR10010
- Ghani, W. A. W. A. K., Mohd, A., da Silva, G., Bachmann, R. T., Taufiq-Yap, Y. H., Rashid, U., and Al-Muhtaseb, A. H. (2013). “Biochar production from waste rubber-wood-sawdust and its potential use in C sequestration: Chemical and physical characterization,” *Ind. Crop. Prod.* 44, 18-24. DOI: 10.1016/j.indcrop.2012.10.017
- Hamzah, Z., Alias, A. A., Hashim, O., and Boonbeng, L. (2013). “Characterization of physicochemical properties of biochar from different agricultural residues,” *Advances in Environmental Biology* 7, 3752-3757.
- Jeong, C. Y., Dodla, S. K., and Wang, J. J. (2016). “Fundamental and molecular composition characteristics of biochars produced from sugarcane and rice crop residues and by-products,” *Chemosphere* 142, 4-13. DOI: 10.1016/j.chemosphere.2015.05.084
- Jin, J., Sun, K., Wang, Z., Han, L., Du, P., Wang, X., and Xing, B. (2017). “Effects of chemical oxidation on phenanthrene sorption by grass- and manure-derived biochars,” *Sci. Total Environ.* 598, 789-796. DOI: 10.1016/j.scitotenv.2017.04.160
- Jindo, K., Mizumoto, H., Sawada, Y., Sanchez-Monedero, M. A., and Sonoki, T. (2014). “Physical and chemical characterization of biochars derived from different agricultural residues,” *Biogeosciences* 11, 6613-6621. DOI: 10.5194/bg-11-6613-2014
- Knicker, H., Totsche, K. U., Almendros, G., and González-Vila, F. J. (2005). “Condensation degree of burnt peat and plant residues and the reliability of solid-state VACP MAS ¹³C NMR spectra obtained from pyrogenic humic material,” *Org. Geochem.* 36(10), 1359-1377. DOI: 10.1016/j.orggeochem.2005.06.006
- Lee, J. W., Kidder, M., Evans, B. R., Paik, S., Buchanan, A. C., Garten, C. T., and Brown, R. C. (2010). “Characterization of biochars produced from cornstovers for soil amendment,” *Environ. Sci. Technol.* 44(20), 7970-7974. DOI: 10.1021/es101337x
- Lehmann, J., Gaunt, J., and Rondon, M. (2006). “Bio-char sequestration in terrestrial

- ecosystems - A review,” *Mitig. Adapt. Strat. Gl.* 11(2), 403-427. DOI: 10.1007/s11027-005-9006-5
- Lith, S. C. V., Alonsoramírez, V., Jensen, P. A., And, F. J. F., and Glarborg, P. (2006). “Release to the gas phase of inorganic elements during wood combustion. Part 1: Development and evaluation of quantification methods,” *Energy & Fuels* 20(3), 964-978.
- Lith, S. C. V., Jensen, P. A., Frandsen, F. J., and Glarborg, P. (2008). “Release to the gas phase of inorganic elements during wood combustion. Part 2: Influence of fuel composition,” *Energy & Fuels* 22(3), 1598-1609.
- Magdziarz, A., and Werle, S. (2014). “Analysis of the combustion and pyrolysis of dried sewage sludge by TGA and MS,” *Waste Manage.* 34(1), 174-179. DOI: 10.1016/j.wasman.2013.10.033
- Murali, S., Shrivastava, R., and Axena, M. (2010). “Green house gas emissions from open field burning of agricultural residues in India,” *J. Environ. Sci. Eng.* 52(4), 277-284.
- Niu, W., Han, L., Liu, X., Huang, G., Chen, L., Xiao, W., and Yang, Z. (2016). “Twenty-two compositional characterizations and theoretical energy potentials of extensively diversified China’s crop residues,” *Energy* 100, 238-250. DOI: 10.1016/j.energy.2016.01.093
- Pastorova, I., Botto, R. E., Arisz, P. W., and Boon, J. J. (1994). “Cellulose char structure: A combined analytical Py-GC-MS, FTIR, and NMR study,” *Carbohydr. Res.* 262(1), 27-47. DOI: 10.1016/0008-6215(94)84003-2
- Peng, C., Luo, H., and Kong, J. (2014). “Advance in estimation and utilization of crop residues resources in china,” *Chinese Journal of Agricultural Resources and Regional Planning.* DOI: 10.7621/cjarrp.1005-9121.20140303
- Pituello, C., Francioso, O., Simonetti, G., Pisi, A., Torreggiani, A., Berti, A., and Morari, F. (2015). “Characterization of chemical–physical, structural and morphological properties of biochars from biowastes produced at different temperatures,” *J. Soils Sediments* 15(4), 792-804. DOI: 10.1007/s11368-014-0964-7
- Quilliam, R. S., Glanville, H. C., Wade, S. C., and Jones, D. L. (2013). “Life in the 'charosphere' - Does biochar in agricultural soil provide a significant habitat for microorganisms?,” *Soil Biol. Biochem.* 65, 287-293. DOI: 10.1016/j.soilbio.2013.06.004
- Sluiter, J. B., Ruiz, R. O., Scarlata, C. J., Sluiter, A. D., and Templeton, D. W. (2010). “Compositional analysis of lignocellulosic feedstocks. 1. Review and description of methods,” *Journal of Agricultural & Food Chemistry* 58(16), 9043.
- Sohi, S., Lopez-Capel, E., Krull, E., and Bol, R. (2009). *Biochar, Climate Change and Soil: A Review to Guide Future Research*, CSIRO, Canberra, Australia.
- Srinivasan, P., and Sarmah, A. K. (2015). “Characterisation of agricultural waste-derived biochars and their sorption potential for sulfamethoxazole in pasture soil: A spectroscopic investigation,” *Sci. Total. Environ.* 502, 471-480. DOI: 10.1016/j.scitotenv.2014.09.048
- Sun, K., Kang, M., Zhang, Z., Jin, J., Wang, Z., Pan, Z., Xu, D., Wu, F., and Xing, B. (2013). “Impact of deashing treatment on biochar structural properties and potential sorption mechanisms of phenanthrene,” *Environ. Sci. Technol.* 47(20), 11473-11481. DOI: 10.1021/es4026744
- Taherymoosavi, S., Joseph, S., and Munroe, P. (2016). “Characterization of organic compounds in a mixed feedstock biochar generated from Australian agricultural

- residues,” *Journal of Analytical & Applied Pyrolysis* 120, 441-449.
- Venegas, A., Rigol, A., and Vidal, M. (2015). “Viability of organic wastes and biochars as amendments for the remediation of heavy metal-contaminated soils,” *Chemosphere* 119, 190-198. DOI: 10.1016/j.chemosphere.2014.06.009
- Villamil, M. B., Little, J., and Nafziger, E. D. (2015). “Corn residue, tillage, and nitrogen rate effects on soil properties,” *Soil Till. Res.* 151, 61-66. DOI: 10.1016/j.still.2015.03.005
- Wiedner, K., Fischer, D., Walther, S., Criscuoli, I., Favilli, F., Nelle, O., and Glaser, B. (2015). “Acceleration of biochar surface oxidation during composting?,” *J. Agr. Food Chem.* 63(15), 3830-3837. DOI: 10.1021/acs.jafc.5b00846
- Wu, F., Jia, Z., Wang, S., Chang, S. X., and Startsev, A. (2013). “Contrasting effects of wheat straw and its biochar on greenhouse gas emission and enzyme activities in a chernozemic soil,” *Biol. Fert. Soils* 49(5), 555-565. DOI: 10.1007/s00374-012-0745-7
- Wu, W., Yang, M., Feng, Q., McGrouther, K., Wang, H., Lu, H., and Chen, Y. (2012). “Chemical characterization of rice straw-derived biochar for soil amendment,” *Biomass Bioenerg.* 47, 268-276. DOI: 10.1016/j.biombioe.2012.09.034
- Xiao, X., Chen, Z., and Chen, B. (2016). “H/C atomic ratio as a smart linkage between pyrolytic temperatures, aromatic clusters and sorption properties of biochars derived from diverse precursory materials,” *Sci. Rep.-UK* 6, 1-13. DOI: 10.1038/srep22644
- Yang, F., Zhao, L., Gao, B., Xu, X., and Cao, X. (2016). “The interfacial behavior between biochar and soil minerals and its effect on biochar stability,” *Environ. Sci. Technol.* 50(5), 2264-2271. DOI: 10.1021/acs.est.5b03656
- Yao, Y., Gao, B., Inyang, M., Zimmerman, A. R., Cao, X., Pullammanappallil, P., and Yang, L. (2011). “Biochar derived from anaerobically digested sugar beet tailings: Characterization and phosphate removal potential,” *Bioresource Technol.* 102(10), 6273-6278. DOI: 10.1016/j.biortech.2011.03.006
- Yargicoglu, E. N., Sadasivam, B. Y., Reddy, K. R., and Spokas, K. (2015). “Physical and chemical characterization of waste wood derived biochars,” *Waste Manage.* 36, 256-268. DOI: 10.1016/j.wasman.2014.10.029
- Yuan, J.-H., Xu, R.-K., and Zhang, H. (2011). “The forms of alkalis in the biochar produced from crop residues at different temperatures,” *Bioresource Technol.* 102(3), 3488-3497. DOI: 10.1016/j.biortech.2010.11.018
- Zhang, H., Voroney, R. P., and Price, G. W. (2015a). “Effects of temperature and processing conditions on biochar chemical properties and their influence on soil C and N transformations,” *Soil Biol. Biochem.* 83, 19-28. DOI: 10.1016/j.soilbio.2015.01.006
- Zhang, J., Liu, J., and Liu, R. (2015b). “Effects of pyrolysis temperature and heating time on biochar obtained from the pyrolysis of straw and lignosulfonate,” *Bioresource Technol.* 176, 288-291. DOI: 10.1016/j.biortech.2014.11.011
- Zhang, W., Nefedov, A., Naboka, M., Cao, L., and Wöll, C. (2012). “Molecular orientation of terephthalic acid assembly on epitaxial graphene: NEXAFS and XPS study,” *Phys. Chem. Chem. Phys.* 14(29), 10125-10131. DOI: 10.1039/C2C923748B

Article submitted: November 1, 2017; Peer review completed: December 30, 2017;
Revised version received: January 16, 2018; Accepted: February 19, 2018; Published:
March 20, 2018. DOI: 10.15376/biores.13.2.3429-3446